JOURNAL OF MATERIALS SCIENCE 21 (1986) 117–122

Crystallization kinetics of Zr–33 at% Ni amorphous alloy

G. K. DEY, E. G. BABURAJ, S. BANERJEE
Physical Metallurgy Division, Bhabha Atomic Research Centre, Trombay, Bombay 400 085, India

The amorphous to crystalline transition in Zr–33 at% Ni amorphous alloy has been found to occur by polymorphic crystallization. The product of the cyrstallization process has been identified as the equilibrium Zr_2Ni intermetallic phase. The kinetics of crystallization have been studied independently using differential scanning calorimetry (DSC) and transmission electron microscopy. The activation energy of crystallization has been evaluated by isothermal and continuous heating in DSC. The isothermal anneals have revealed that the crystallization follows the Johnson–Mehl–Avrami kinetics with an Avrami exponent close to 4. The microstructural changes accompanying crystallization have been studied for an interpretation of the Avrami exponent. The nucleation and growth rates of crystals have been estimated at different temperatures in order to determine the activation energies of the two processes. It has been found that nucleation is thermally activated and growth is interface-controlled.

1. Introduction

Polymorphic crystallization [1] has been observed in metal–metal as well as metal–metalloid glasses [2, 3]. The complexities associated with isothermal kinetics studies in specimens undergoing only polymorphic or eutectic cyrstallization are less as compared to specimens undergoing primary crystallization, due to the fact that a single isothermal exotherm characterizing the processes is obtained in DSC in the former two cases. Primary crystallization is always accompanied by either eutectic or polymorphic crystallization [1] and this makes it difficult to study the primary crystallization process independently. Complementary microstructural studies performed to substantiate the findings of the DSC investigations are simpler in polymorphic crystallization as compared to eutectic crystallization, since the former involves the formation of a single crystallization phase. It is surprising that in spite of these factors not many complete characterization studies of crystallization kinetics, making use of DSC and supplementary microstructural examinations, have been reported for polymorphic crystallization.

This paper deals with polymorphic crystallization in a Zr–33 at% Ni amorphous alloy. The kinetics of crystallization have been independently examined by DSC and transmission electron microscopy for an overall understanding of the process. The validity of the formulation relating the activation energies of nucleation, growth and of the total process, has also been examined in the context of this amorphous alloy. Though Scott *et al.* [2] have investigated the crystallization of this amorphous alloy earlier, their studies did not include isothermal DSC investigation.

2. Experimental details

High-purity nickel and crystal-bar zirconium were melted under a pure argon atmosphere in an arc furnace to obtain alloy buttons. The buttons were remelted several times for homogenization. Pieces of the alloy button were melt-spun in a melt-spinning device incorporating a 20 cm diameter copper disc to obtain ribbons about 25 μm thick and 4 mm wide. A protective argon atmosphere was used during melt-spinning.

Differential scanning calorimetry was carried out in a Perkin Elmer DSC II unit. Thin foils for electron microscopy were prepared by using an electrolyte containing 300 ml of methanol, 30 ml of perchloric acid and 170 ml of n-butanol. The electrolyte temperature was maintained below 220 K by using a bath containing a dry ice–methanol mixture.

3. Results

3.1. Differential scanning calorimetry

3.1.1. Continuous heating

Thermograms obtained by continuous heating of the amorphous specimens at different heating rates (2.5, 5, 10, 20, 40 and 80 K min^{-1}) showed a single exotherm (Fig. 1). The activation energy of crystallization was estimated by using the expression due to Kissinger [4]:

$$\ln\left(\frac{C}{T_p^2}\right) = \frac{-E_c}{RT_p} + A \qquad (1)$$

where C is the heating rate, T_p is the peak temperature, E_c is the activation energy and R and A are constants. The slope of the plot of $\ln (C/T_p^2)$ against $1/T_p$ (Fig. 2) gave an activation energy value of 319 kJ mol^{-1}.

3.1.2. Isothermal kinetics

Isothermal kinetics were studied in the temperature range 670 to 680 K. At temperatures below 670 K the incubation period was excessively long and the exotherms tended to flatten out. Studies could not be

0022–2461/86 $03.00 + .12

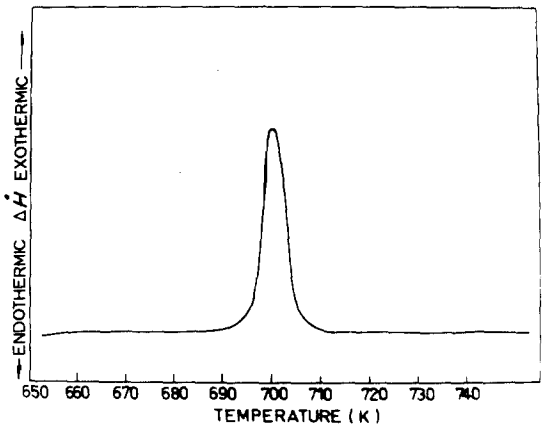

Figure 1 DSC thermogram showing a single exotherm obtained at a heating rate of 20 K min^{-1}. $\Delta\dot{H}$ indicates the rate of heat flow.

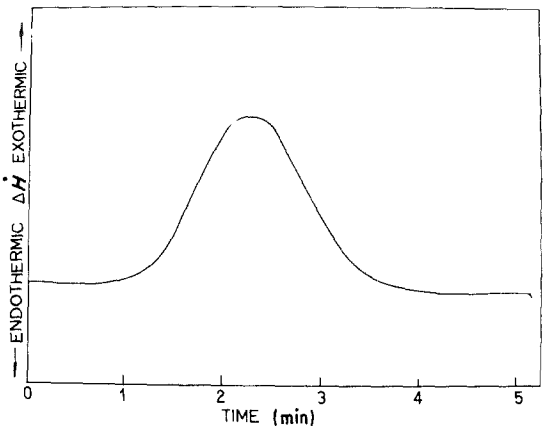

Figure 3 A typical exotherm obtained during isothermal annealing in DSC.

performed at temperatures higher than 680 K because of the frequently encountered difficulty of the incubation time falling short of the instrument transient time. A typical isothermal exotherm is shown in Fig. 3. The crystallization kinetics were analysed in terms of the Johnson–Mehl–Avrami relationship [5]

$$x = 1 - \exp(-bt^n) \quad (2)$$

where x is the fraction transformed in time t, b is a rate constant and n is the Avrami exponent. The fraction transformed, x, at any time t was determined as the ratio $A(t)/A(\text{tot})$ where $A(t)$ and $A(\text{tot})$ respectively stand for the area under the isothermal exotherm up to time t and the total area of the exotherm. Sigmoidal curves (Fig. 4) were obtained by plotting x against at different temperatures. The Avrami exponent was estimated from the slope of plots of $\log[-\log(1 - x)]$ against $\log t$ (Fig. 5). These estimated values of the Avrami exponent for different temperatures are listed in Table I.

The activation energy of crystallization was determined from the isothermal exotherm making use of the Arrhenius relation

$$t_{0.5} = t_0 \exp(E_c/RT) \quad (3)$$

where $t_{0.5}$ is the time for completion of 50% transformation. The slope of plots of $\log t_{0.5}$ against $1/T$ (Fig. 6) yielded an activation energy value of 314 kJ mol^{-1}.

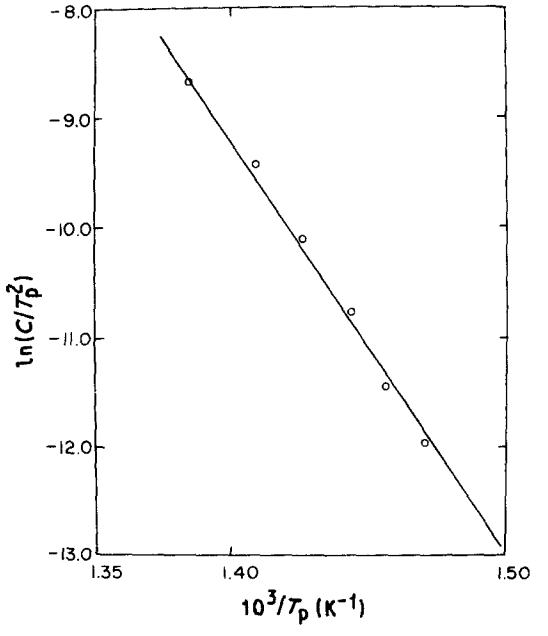

Figure 2 Plot of $\ln C/T_p^2$ against $1/T$ to estimate the activation energy of crystallization by Kissinger's method.

3.2. X-ray diffraction

Conventional X-ray diffraction was used to characterize the amorphous structure and to identify the crystalline phase forming on crystallization. The solidified amorphous structure showed a broad maximum at $4\pi\text{Sin}\,\theta/\lambda = 25.7\,\text{nm}^{-1}$ using Cu$K\alpha$ radiation. The specimens continuously heated beyond the exotherm in DSC and specimens annealed at 623 K for 8 h were found to contain the Zr_2Ni phase which has a C16 structure [6]. The lattice parameters of this phase were found to be $a = 0.6470$ nm and $c = 0.5240$ nm. No other crystalline phase could be detected.

3.3. Transmission electron microscopy

TEM studies were performed for a quantitative estimation of nucleation and growth rates of crystals at different temperatures, and for a detailed morphological study of the crystals forming in the amorphous matrix.

The crystals formed in specimens annealed at 623 K for 3 h were found to have irregular shapes and contained a fine internal structure (Fig. 7). Electron diffraction patterns from the crystals (Fig. 8) could be interpreted in terms of reciprocal lattice sections of the Zr_2Ni phase. Streaking was observed along the [1 1 0] direction, indicating either faulting or small size of the diffracting domains along these directions. However, the possibility that each crystal consisted of many

TABLE I Avrami exponent values at different temperatures

Temperature (K)	Avrami exponent
672.0	3.52
673.5	3.20
675.0	3.38
677.0	4.12
679	3.73

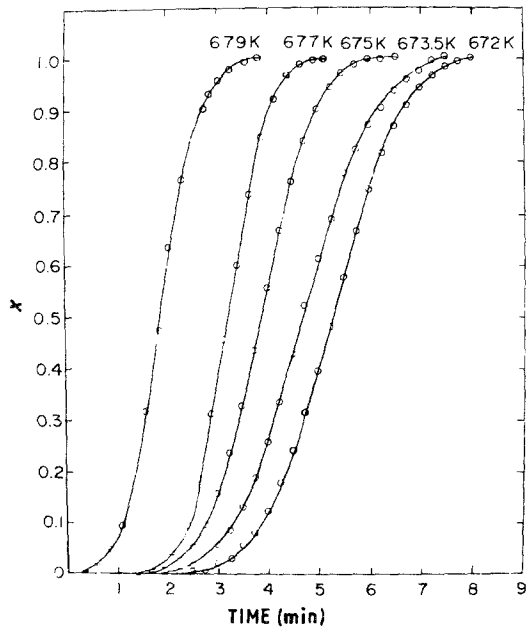

Figure 4 Sigmoidal plots of fraction transformed against time elapsed at different temperatures.

small crystallites was ruled out in view of the fact that the electron diffraction patterns were typical of single crystals.

The rates of nucleation were studied in specimens annealed at 610, 620, 630 and 640 K. The nucleation rates were estimated by counting the number of crystals per unit volume of TEM foil with suitable corrections for sectioning. The nucleation density was found to increase linearly with time at all these temperatures.

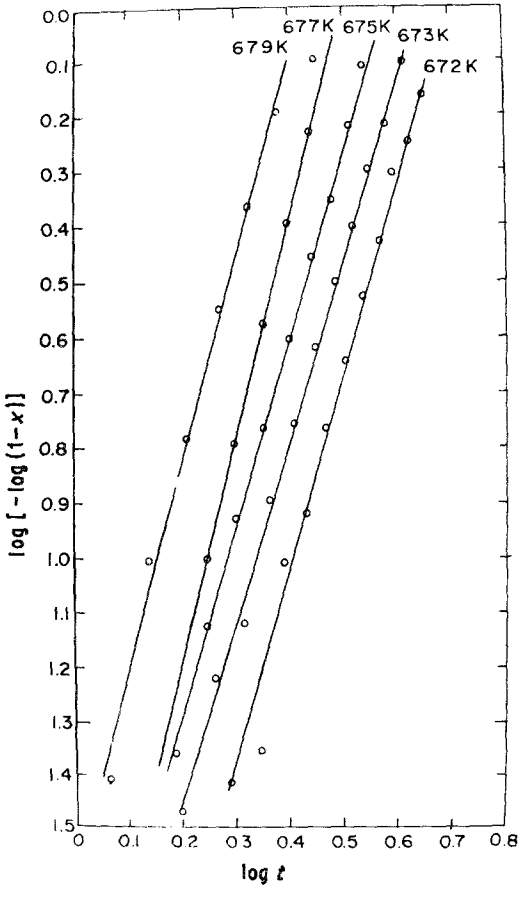

Figure 5 Plots of determination of Avrami exponent.

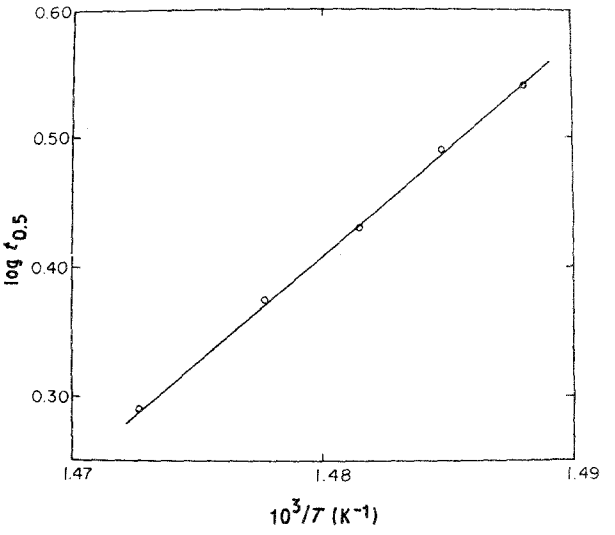

Figure 6 Plots for determination of the activation energy of crystallization from isothermal annealing data. $t_{0.5}$ represents time for 50% transformation.

The results of the nucleation rate estimations are shown in Fig. 9.

The steady-state nucleation rate given by Becker–Volmer nucleation theory [7] is

$$\dot{N} = N_0 \exp\left(-\frac{\Delta G_c}{RT}\right)\exp\left(\frac{-Q_n}{RT}\right) \quad (4)$$

where N_0 is a constant, ΔG_c is the free energy per mole of nucleation and Q is the activation for atomic transport to an embryo. On incorporating the activation energy of nucleation Q_n (the sum of ΔG_c and Q) Equation 4 reduces to the form

$$\dot{N} = N_0 \exp\left(-\frac{Q_n}{RT}\right) \quad (5)$$

The activation energy of nucleation was estimated from the slope of plot of ln N against $1/T$ (Fig. 10) and was found to be 600 kJ mol^{-1}.

The growth rates were estimated by measuring the size of the largest crystal in each specimen. The growth rate at each temperature was found to be constant. The results of growth rate measurements are shown in Fig. 11. The growth of the crystals was isotropic and did not show any faceting tendency. The crystal size distribution was found to be wide and was hence suggestive of the operation of a homogeneous nucleation process. This mode of growth and this kind of crystal size distribution were observed in all specimens.

The growth rate of the crystals is given by the following expression [8]:

$$\dot{G} = \nu\delta \exp\left(-\frac{Q_g}{RT}\right)\left[1 - \exp\left(-\frac{\Delta G}{RT}\right)\right] \quad (6)$$

where ΔG is the change in chemical free energy per mole accompanying crystallization, Q_g is the activation energy for growth, ν is a characteristic frequency and δ is the interface width. At small valves of T, typical of the crystallization of metallic glasses, $\Delta G \gg RT$ and the equation reduces to the form

$$\dot{G} = \nu\delta \exp\left(-\frac{Q_g}{RT}\right) \quad (7)$$

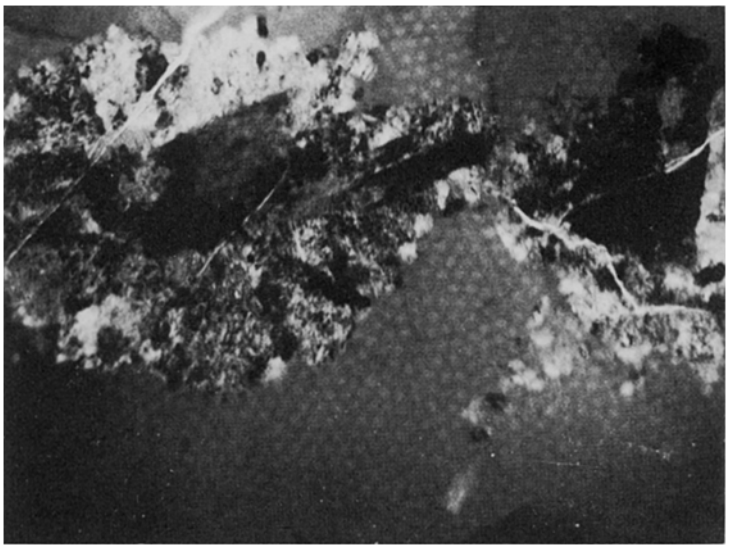

Figure 7 Crystal of Zr_2Ni in an amorphous matrix. The crystal has a fine internal structure. Note the mottled contrast in the amorphous matrix. Bright-field micrograph.

The activation energy of growth was determined by estimating the slope of plots of $\ln \dot{G}$ against $1/T$ (Fig. 12) and was found to be 208 kJ mol^{-1}.

A mottled constrast which might be supposed to represent phase separation was observed in amorphous regions of some of the specimens after annealing (Fig. 7). However, chemically thinned specimens did not show mottled contrast. Thin foils of as-solidified ribbons prepared by electropolishing also did not show any mottled contrast (Fig. 13).

4. Discussion

Structural investigations of the amorphous structure, using X-ray and electron diffraction, indicated the presence of a single amorphous phase. Contrast typical of phase separation observed in the amorphous region in some of the partially crystalline specimens seems to have originated due to a non-uniform attack by the electrolyte. In this regard, Dong *et al.* [9] have also arrived at the same conclusion. Crystallization in the Zr-33% Ni amorphous alloy involved the transformation of the amorphous phase to a single crystalline phase of the same composition, which according to the terminology of Koster and Herold [1] is polymorphic crystallization.

The observation of a single exotherm during continuous heating was in conformity with the operation of a single-step crystallization process. A single exotherm would also be obtained in a situation where simultaneous formation of more than one crystalline phase occurs. However, microstructural investigations confirmed the formation of a single phase in the present case. It can be mentioned in this context that two exotherms are obtained in a more nickel-rich amorphous alloy (Zr–39 at % Ni), the first due to the formation of a Zr_2Ni phase and the second due to the emergence of the ZrNi phase [10].

A comparison of the activation energy estimated by Kissinger's method with that determined by isothermal experiments revealed a good agreement between the two (319 and 314 kJ mol^{-1}), as has been observed in all such instances [11, 12].

4.1. Nucleation

Athermal as well as thermally activated nucleation of crystals are known to occur in metallic glasses. Athermal nucleation is brought about by the growth of quenched-in nuclei which form during rapid solidification. Crystallization effected solely by the growth of athermal nuclei is marked by a very narrow size

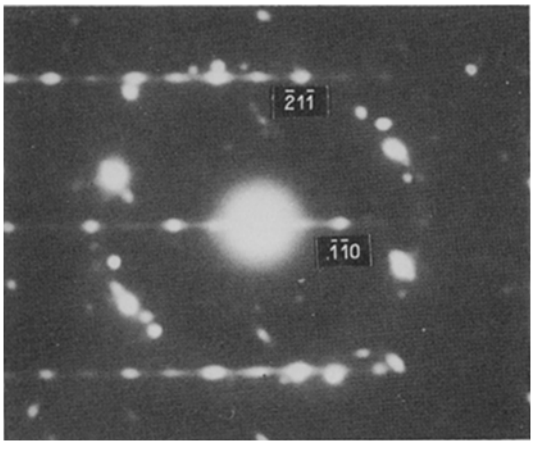

Figure 8 Electron diffraction pattern from the Zr_2Ni crystal. Streaking along the [1 1 0] direction can be seen.

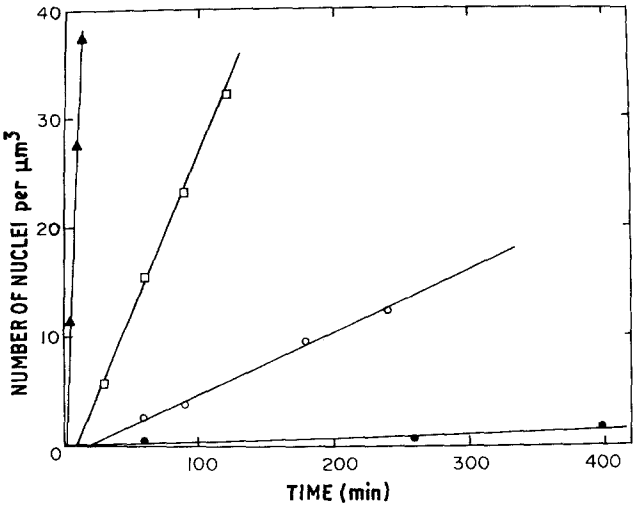

Figure 9 Plots of nucleus density against time. Nucleation rates are contrast at each temperature. (●) 610 K, (○) 620 K, (□) 630 K, (△) 640 K.

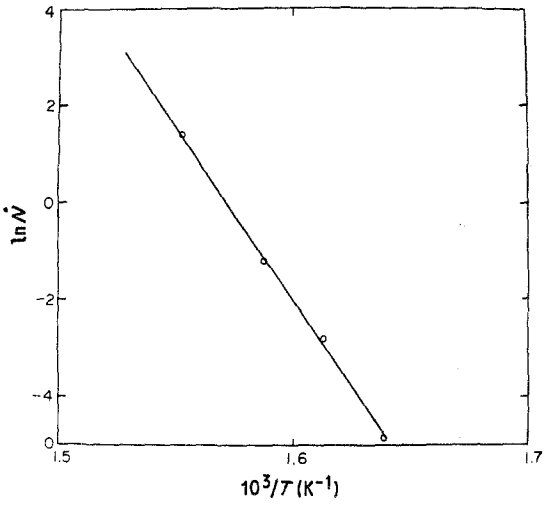

Figure 10 Plot for estimation of the activation energy of nucleation.

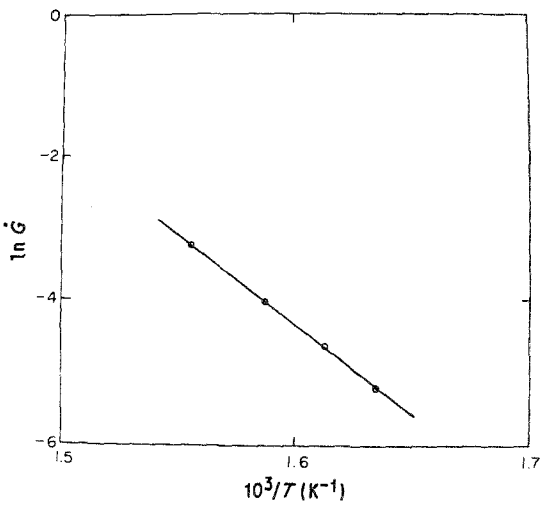

Figure 12 Plot for estimation of the activation energy of growth.

distribution of the crystallites [3, 13]. In addition, since the nucleation process does not require any thermal activation, the activation energy of the overall process equals the activation energy of growth. The observed wide size distribution of crystallites and the fact that the activation energy of growth (208 kJ mol^{-1}) was much smaller than the activation energy of the overall process (314 to 319 kJ mol^{-1}) indicated a very meagre participation of quenched-in nuclei in the crystallization process. That thermally activated nucleation was the main nucleation mechanism was also supported by the observation of well-defined incubation periods at all isothermal annealing temperatures (Fig. 4). The incubation time is a manifestation of the transient period during which the steady-state thermally activated nucleation rate is established. The nucleation rate at all temperatures was found to be independent of time, as has been observed in other cases of polymorphic crystallization [2, 14].

4.2. Growth

The growth of the crystals was found to be isotropic, i.e. the rate of growth was almost identical along the different crystallographic directions. In several amorphous alloys, polymorphic crystallization has been found to occur by the formation of faceted crystals [1, 13]. The faceted morphology results from stepwise or anisotropic growth. In some instances a transition from a faceted to a isotropic growth mode has also been observed [13]. No transition from isotropic to faceted growth was, however, observed in the present case.

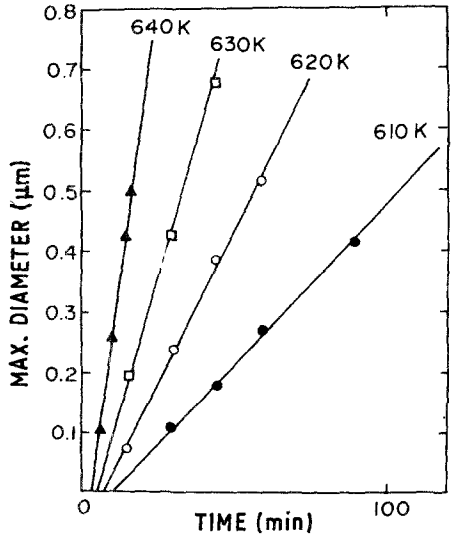

Figure 11 Plots showing the time dependence of the diameter of Zr_2Ni crystals at different temperatures.

The activation energy of growth during polymorphic crystallization signified the activation required for atomic jumps across the crystal–amorphous matrix interface. The value obtained in the present case is lower than that observed for polymorphic crystallization in some metal–metalloid glasses [14].

The activation energy of the crystallization process determined by DSC and the activation energies of nucleation and growth of crystals determined by TEM in this study were all in good agreement with those estimated by Scott and co-workers [2, 9].

A spread in the value of the Avrami exponent evaluated for different annealing temperatures has been observed in almost all previous crystallization studies [11, 12]. The variation in the value of the Avrami exponent observer over the temperature range in this study compares very favourably with that observed in other studies [11, 12]. An Avrami exponent value of 4 represents a process involving nucleation at a constant rate and with interface-controlled three-dimensional growth [8]. The nucleation rate observed was constant with time at all temperatures. The growth was three-dimensional (isotropic) and the growth rate was also found to be constant at the temperatures of observation. A constant growth rate is generally observed in interface-controlled processes [8].

The validity of the empirical relationship between Q_n, Q_g and E_c proposed by Ranganathan and Von Heimendahl [15] was examined. For polymorphic crystallization (constant nucleation rate and three-dimensional growth) the relationship assumes the following form:

$$E_c = \frac{Q_n + 3Q_g}{4} \tag{8}$$

Using the experimentally estimated values for Q_n and

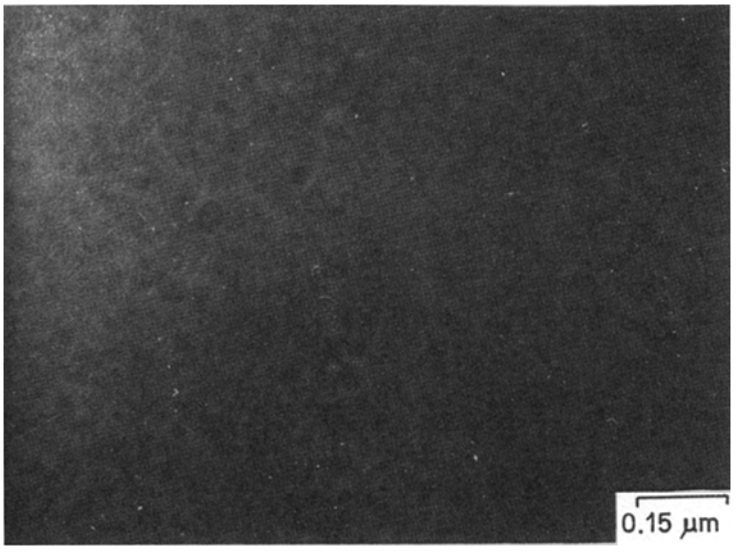

Figure 13 Bright-field micrograph showing the amorphous structure in an unannealed specimen.

Q_g, E_c was found to be 306 kJ mol^{-1} in very good agreement with that obtained by calorimetry. It may be mentioned here that the validity of Equation 8 had not been examined earlier in the case of metal–metal glasses. Ranganathan and Von Heimendahl [15] had examined its validity in the case of metal–metalloid glasses. The present study shows that it is equally valid for metal–metal glasses.

5. Conclusion

Crystallization in the amorphous alloy Zr–33 at % Ni is polymorphic and follows Johnson–Mehl–Avrami kinetics with an Avrami exponent value close to 4. Microstructural examination confirmed the suggested nucleation and growth behaviour from this exponent, i.e. nucleation at constant rate and interface-controlled growth. It was found that during crystallization of this alloy nucleation is thermally activated and growth is isotropic.

Acknowledgements

It is a pleasure to acknowledge the benefit of several discussions the authors had with Dr P. Ramachandra Rao. The authors thank Dr M. K. Asundi for his keen interest in this work, and are grateful to Dr P. Mukhopadhyay for a critical reading of the manuscript.

References

1. U. KOSTER and U. HEROLD, "Topics in Applied Physics", Vol. 46 (Springer Verlag, New York, 1980) p. 225.
2. M. G. SCOTT, G. GREGAN and Y. D. DONG, Proceedings of the 4th International Conference on Rapidly Quenched Metals, Sendai, 1981, (Japan Institute of Metals, Sendai, 1982) p. 671.
3. U. KOSTER and U. HEROLD, Proceedings of the 4th International Conference on Rapidly Quenched Metals, Sendai, 1981 (Japan Institute of Metals, Sendai, 1982) p. 717.
4. H. E. KISSINGER, *Anal. Chem.* **29** (1957) 1702.
5. J. BURKE, The Kinetics of Phase Transformation in Metals and Alloys" (Pergamon Press, Oxford, 1965) p. 433.
6. J. C. GACHON, M. DIRAND and J. HERTZ, *J. Less-Common Metals* **92** (1983) 307.
7. M. E. FINE, "Introduction to Phase Transformations in Condensed Systems" (MacMillan, London, 1964) p. 14.
8. J. W. CHRISTIAN, "The Theory of Transformations in Metals and Alloys" (Pergamon Press, Oxford, 1965) p. 433.
9. Y. D. DONG, G. GREGAN and M. G. SCOTT, *J. Non-Cryst. Solids* **43** (1981) 403.
10. G. K. DEY and S. BANERJEE, Proceedings of 5th International Conference on Rapidly Quenched Metals, Wurzburg, 1984 (Elsevier, Amsterdam, 1985) p. 345.
11. M. G. SCOTT and P. RAMACHANDRA RAO, *Mater. Sci. Eng.* **29** (1977) 137.
12. E. G. BABURAJ, G. K. DEY, M. J. PATNI and R. KRISHNAN, *Scripta Metall.* **19** (1985) 305.
13. U. KOSTER, "Phase Transformations in Crystalline and Amorphous Alloys", edited by B. L. Mordike (Deutsche Gasellschaft fur Metallkunde, Oberussel, 1983) p. 113.
14. S. RANGANATHAN, J. C. CLAUS, R. S. TIWARI and M. V. HEIMENDAHL, Proceedings of Conference on Metallic Glasses: Science and Technology, Budapest, 1980, Vol. I, p. 327.
15. S. RANGANATHAN and M. VON HEIMENDAHL, *J. Mater. Sci.* **16** (1981) 2401.

Received 27 November 1984
and accepted 28 February 1985